Title	Tailoring lanthanide nanocrystals for nanomedicine
Author(s)	Zhang, Yan; Tan, Thatt Yang Timothy
Citation	Zhang, Y., & Tan, T. Y. T. (2013). Tailoring lanthanide nanocrystals for nanomedicine. Progress in Biomedical Optics and Imaging - Proceedings of SPIE, 8595.
Date	2013
URL	http://hdl.handle.net/10220/12911
Rights	© 2013 SPIE. This paper was published in Progress in Biomedical Optics and Imaging - Proceedings of SPIE and is made available as an electronic reprint (preprint) with permission of SPIE. The paper can be found at the following official DOI: [http://dx.doi.org/10.1117/12.2006288]. One print or electronic copy may be made for personal use only. Systematic or multiple reproduction, distribution to multiple locations via electronic or other means, duplication of any material in this paper for a fee or for commercial purposes, or modification of the content of the paper is prohibited and is subject to penalties under law.

Tailoring Lanthanide Nanocrystals for Nanomedicine

Yan Zhang and Timothy T.Y. Tan*
School of Chemical and Biomedical Engineering
Nanyang Technological University, Singapore

ABSTRACT

Lanthanide nanocrystals have demonstrated strong potentials in nanomedicine due to its up-conversion and strong magnetic properties, and low toxicity. This talk will focus on strategies in lanthanide nanostructure tailoring to achieve up-conversion color emission tuning, MRI T_1 and T_2 contrast tuning, and the use of up-conversion fluorescence in drug delivery and cancer cells ablation.

Keywords: Lanthanide, nanocrystals, magnetic resonance imaging, up-conversion fluorescence, drug delivery, cancer cells ablation， nanomedicine.

1. INTRODUCTION

Nanomedicine is an emerging field that applies nanotechnology into medicine, mainly advanced diagnostics (imaging) and therapeutics (drug delivery and target therapy).[1] Over the past decade, there has been an explosive development of nanosystems designed for purposes from diagnosis to treatment of various types of diseases including cancer. These systems, such as dendrimers, gold nanoparticles, organic-inorganic hybrid, compared with traditional molecule-based drug, enable a highly integrated design that incorporate multiple functions, such as intelligent drug delivery, imaging devices or as medical sensors to detect and diagnose disease, into one system.[2, 3] As such, early and accurate diagnosis coupled with on-site delivery and treatment using suitable therapeutic agents at the early stage of the disease will facilitate timely clinical intervention and can mitigate patient risk and disease progression.

In nanomedicine, molecular imaging is important as it provides visualizing, characterizing and monitoring the abnormalities or biological processes at the molecular and cellular level.[4, 5] It offers great potential in detecting molecular and cellular changes caused by the disease before the abnormalities are large enough to cause change in the anatomical structure that can be detected by the imaging modalities. Various imaging modalities (e.g. positron emission tomography (PET), single photon emission computed tomography (SPECT), magnetic resonance imaging (MRI), optical, ultrasound) have been widely used clinically to understand and diagnose various diseases.[6] MRI, for example, has become a prominent clinical imaging technique as it can provide highly resolved 3-dimentional imaging of whole body and soft tissue contrast, therefore, distinguish pathological tissues from normal tissues. It provides high spatial resolution and depth for *in vivo* imaging. Moreover, it is non-invasive, fast and avoids the use of ionizing radiation or radiotracers, therefore, it is harmless to the patient. However, it suffers from low sensitivity.[6] Optical imaging, on the contrary, has high sensitivity but suffers from low tissue penetration depths.[7] Every imaging modality has its own advantages and disadvantages and no single technique possesses the full capacities to obtain comprehensive and accurate biological information. Hence, multimodal imaging, where several detection techniques can be combined and visualized, is clearly attractive as it combines the strengths of each imaging modality while offsetting the limitations of others, ensuring more accurate and reliable data.[8] Contrast agents are generally used in imaging modalities to help identify particular biomarkers or pathways with high sensitivity and selectivity. Multifunctional nanomaterials, considering their compatible sizes, intrinsic physic/chemical properties and ease of integrating multiple functions, hold great promise for future therapeutic applications.

In this regard, lanthanide nanocrystals (NCs) have received ubiquitous attentions over the past decades. Lanthanide is a series comprising of fifteen elements in the periodic table ranging from lanthanum to lutetium. They have a general electronic configuration, with minor exceptions $[Xe]6s^2 4f^n$ with n=0 (La) to 14 (Lu) and their most stable oxidation state is +3 with a $[Xe]\ 4f^n$ configuration. These 4f orbitals are shielded from the atom's environment by the 5s and 5p electrons. Consequently, they exhibit unique fluorescent and magnetic properties.

*Correspondence: Email: tytan@ntu.edu.sg; Telephone: (+65)6316 8829; Fax: (65) 6794 7553

Colloidal Nanocrystals for Biomedical Applications VIII, edited by Wolfgang J. Parak, Marek Osinski, Kenji Yamamoto, Proc. of SPIE Vol. 8595, 859516 · © 2013 SPIE
CCC code: 1605-7422/13/$18 · doi: 10.1117/12.2006288

Lanthanides exhibit sharp and intense fluorescence and exhibit several unique characteristics as follow: (i) a much longer emission lifetime compared to other fluorescent agents such as dyes, fluorescent protein and QDs (μs to ms), which help to diminish spontaneous background fluorescence from the biological specimen; (ii) the emission intensity can be tuned by changing the type of host matrix, dopant and dopant concentration; (iii) multicolor luminescence can be easily realized by varying the dopant and host matrix. Moreover, unlike the size-dependent emission of QDs, the emission of lanthanide ions is not sensitive to particle size; (iv) up-conversion (UC) luminescence from Er^{3+}, Tm^{3+} and Ho^{3+} etc can be realized besides common down-conversion (DC) behavior.[9] UC fluorescence is a process that converts two or more low energy photons, usually NIR to high-energy emission through sequential absorption and energy transfer steps. It provides tremendous advantages compared to DC emission when it comes to biomedical application due to the following reasons: (i) longer-wavelength NIR emissions are more efficient in penetrating the human tissue than visible light, therefore, resulting in significantly lower background autofluorescence from tissues.[9] Other advantages of adopting UC fluorescence in bioimaging include reduced light scattering, photobleaching, and photodamage to biological specimens; (ii) it allows *in vivo* observation with high spatial resolution; (iii) it can be induced by a low cost NIR diode laser source for the generation of simultaneous two-photon process by single wavelength excitation (980 nm).[10] In addition, owing to their small physical dimensions and biocompatibility, lanthanide UCNCs can be easily coupled to proteins or other biological macromolecular systems and used in a variety of assay formats ranging from bio-detection to cancer therapy. Therefore, they have been regarded as promising alternatives to organic fluorophores and quantum dots for applications in biological assays and medical imaging.

Furthermore, lanthanide ions, such as Gd^{3+}, Dy^{3+}, Pr^{3+}, Sm^{3+}, Ho^{3+}, are paramagnetic and can alter the relaxation of water protons of the nearby tissues, which can potentially be used as contrast agents in MRI and enhance the visualization of MRI signals.[11] The use of MR contrast agents, which usually constitutes paramagnetic species, can enhance the contrast between normal and malignant tissues by greatly enhancing the water proton's longitudinal (T_1) or transverse (T_2) relaxation rate, the effect which is widely known as proton relaxation enhancement (PRE).[12, 13] T_1 contrast agents, which typically comprised of paramagnetic complex containing Gd^{3+} and Mn^{2+} ions, induce bright MR images in T_1-weighted experiments by increasing the spin-lattice relaxation rate of nearby water protons. Gd^{3+}-chelates such as Gd-DTPA (Magnevist®) and Gd(DOTA) (Dotarem®) have a very low toxicity, even at relatively high doses and have been applied in clinical T_1-weighted imaging.[14] T_2 contrast agents which are typically superparamagnetic nanoparticles (NPs) (e.g., iron oxide NPs) or Dy^{3+}-chelates cause protons in their vicinity to undergo fast spin-spin relaxation which gives rise to dark MR images in T_2-weighted experiments.[15, 16]

As such, lanthanide NCs hold great promise as novel contrast agents for both fluorescence imaging and MRI. Through their careful configuration and engineering at nanoscale, they can potentially achieve, simultaneously, efficient detection and imaging, targeting and on-demand drug delivery as well as a non-invasive means of tracking and monitoring the subsequent therapeutic effects.

In this article, we will highlight our recent works in tailoring lanthanide nanostructures to tune UC color emission, MRI T_1 and T_2 contrast tuning, and applying them in drug delivery and cancer cells ablation.

2. TUNING UP-CONVERSION EMISSIONS OF LANTHANIDE NANOCRYSTALS

Each lanthanide ion has a unique set of energy levels and therefore exhibits a set of sharp, distinguishable emission peaks. Tuning their emissions from ultraviolet (UV) to near-infrared (NIR) is quite important to meet their needs in photonics, photovoltaics, biological imaging and therapeutics.[9, 17] Controlling dopant-host combination and dopant concentration are commonly used methods to achieve this purpose.

Varying dopant-host combination is the most straightforward approach to tune the emission colors of UCNCs. The NCs should be photochemical stable, absorb strongly at a given excitation wavelength, and have well-resolved emission spectra with narrow bandwidths. The host lattices are not only needed to closely match the dopant ions but also have low phonon vibration energies so as to decrease the unnecessary cross-relaxation of the dopant. The luminescence from a given lanthanide ion in different host materials may vary considerably due to the different size symmetries of the dopant ions in the various host crystals. By adjusting different combinations of dopant ions and host materials, the emission wavelength and relative intensity of emission peaks can be effectively controlled to modulate emission colors of the lanthanide doped NCs. The most commonly used host lattice for synthesis of lanthanide doped UCNCs are oxides and fluorides. So far, fluorides-based UCNCs (i.e. $NaYF_4$, $NaGdF_4$) have been recognized as one of the most efficient UC

fluorescent hosts due to their low phonon vibration energy. By codoping Yb^{3+}, Er^{3+} /Tm^{3+}/Ho^{3+} ions into the host matrix, they can exhibit different UC emissions.

By choosing appropriate dopant, lanthanides NCs can be tuned to emit in the visible region by using NIR excitation. Using emission in the UV region has significant drawbacks, such as strong background autofluorescence, low detection sensitivity, low light-penetration depth in tissue and high photodamage to the living organisms. Tuning these emissions to generate excitation sources in the visible region can overcome these problems and applying them to excite other semiconductors is an interesting approach with many potential applications, such as up-converting light emitting displays, biological imaging and cancer ablation.[18, 19] Recently, our group has successfully tuned an intense blue emission from Tm^{3+}-doped $NaYF_4$ NCs to excite surface-anchored nitrogen-doped N-TiO_2 NPs, which lead to the generation of highly reactive radical oxygen species (ROS) for cancer cells ablation.[20] NIR-induced drug release and cancer cell killing depend on the UC emission of visible light from $NaYF_4$:Yb,Tm and the light absorbed by the N-TiO_2 semiconductor. To realize efficient energy transfer between the NPs, the photon energy of the emission light should be able to activate electrons from valence band to conduction band and create highly reactive ROS. Tm^{3+} free ions can give emissions at 285 ($^3P_0$-$^3H_6$), 341 ($^3P_0$-$^3F_4$), 365 ($^1D_2$-$^3H_6$), 455 ($^1D_2$-$^3F_4$), 472 ($^1G_4$-$^3H_4$), 645 ($^1G_4$-$^3F_4$) and 800 nm ($^3H_6$ – $^3H_4$). We optimized blue emission by simply varying Tm^{3+} dopant concentration. The mechanism is as shown in Figure 1a. Upon NIR irradiation, Yb^{3+} ions absorb photons due to its large absorption cross section at 970 – 1000 nm and transfer energy to Tm^{3+} ions which later emit blue light with peak centered at 470 nm. N-TiO_2 exhibits obvious absorption at 470 nm, indicating its strong absorption at this wavelength. As shown in Figure 1b, the photoluminescence (PL) intensity of the N-TiO_2/$NaYF_4$:Yb,Tm at blue emission peak of 470 nm (I_{470}) is much lower than that of $NaYF_4$:Yb,Tm. Although the PL intensities of the N-TiO_2/$NaYF_4$:Yb,Tm at 640 nm and 795 nm (I_{795}) also decreased, the reduction of these emission peaks was much stronger than that of the emission peak at 470 nm. The PL intensity ratio of I_{470}/I_{795} for the N-TiO_2/$NaYF_4$:Yb,Tm composite is 0.23, which is much smaller than the value of 0.43 for the pure $NaYF_4$:Yb,Tm, indicating enhanced blue absorption by N-TiO_2.

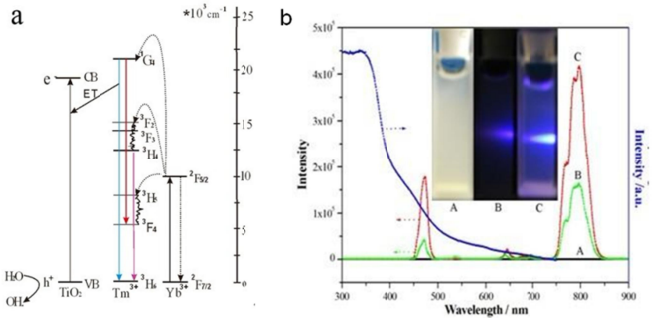

Figure 1. a) Illustration of energy transfer mechanism from NaYF4:Yb,Tm to N-TiO_2 upon NIR excitation. b) Up-conversion emission spectra of: A) N-TiO2; B) N-TiO2/ NaYF4:Yb,Tm; C) NaYF4:Yb,Tm; blue line shows the light absorption spectra of N-TiO2; Inset: photographs showing the light emission of the particle solutions.

In deep tissue imaging, mixed blue/green emissions are not suitable due to the reduced sensitivity from strong absorbance of tissues of short wavelength light below 600 nm. Red (600-700 nm) and NIR spectral range (700-1100 nm) are considered as the "optical windows" for biological tissues, where light scattering, absorbance and autofluorescence of tissues are remarkably reduced due to the absence of endogenous absorber.[21] Recent efforts have been made to synthesis of NCs with single-band UC by involving some metals. These metals act as "tuning" tool. Mn^{2+} ion, for example, has five unpaired d electrons and consists of $^4T_1$ energy states, which can facilitate non-radiative energy transfer from Er^{3+} and energy state to achieve pure emissions. $KMnF_3$, $NaYF_4$ doped with Mn^{2+} ions NCs have been prepared.[21, 22] In our recent work, we exploited sub-10 nm $NaMnF_3$ NCs as ultrasensitive host for pure red and NIR UC fluorescence.[23] Mn^{2+} ions were found to have quenching effect to the luminescence centers. Er^{3+} ions, for instance, they can depopulated energy levels $^2H_{9/2}$ and $^4S_{3/2}$ of Er^{3+} ion to $^4T_1$. In order to optimize the paramagnetic centers, 50 mol% Mn^{2+} ratio was chosen followed by varying Yb^{3+} and Er^{3+}/Tm^{3+} concentrations in the study. When Mn^{2+} concentration was fixed at 50 mol%, the red-to green peak intensity ratio increased significantly with increasing Er^{3+} dopant levels, and a single narrow-band red emission at 660 nm was observed at 50/25/25 mol% Mn^{2+}:Yb^{3+}:Er^{3+} (Figure 2a). This was ascribed to the presence of the $^4T_1$ level in Mn^{2+}, which facilitates nonradiative energy transfer from the $^2H_{9/2}$ and $^4S_{3/2}$ levels of Er^{3+} to the $^4T_1$ level of Mn^{2+}, followed by back energy transfer to the $^4F_{9/2}$ level of Er^{3+}, which returns to the ground state to give red emission (Figure 2c). We also speculated that dopant concentration determined the distance

between the two neighboring activator ions, and high Er^{3+} doping concentration in the NCs facilitates energy transfer between Er^{3+} and Mn^{2+}, which can promote the excited $^4S_{3/2}$ state (responsible for the green emission) from Er^{3+} relaxing further to the lower $^4F_{9/2}$ level, hence leading to the increase of red emission. A pure intense emission at 800 nm was also observed at 50:45:5% Mn^{2+}:Yb^{3+}:Tm^{3+} (Figure 2b), which was ascribed to nonradiative energy transfer from the $^1D_2$ and $^1G_4$ levels of Tm^{3+} to the $^4T_1$ level of Mn^{2+}, followed by back-energy transfer to the $^3F_2$ level of Tm^{3+} (Figure 2d).

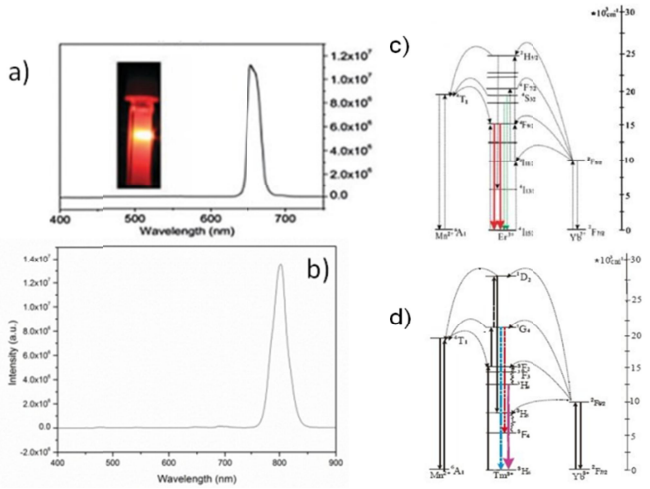

Figure 2. a) Room temperature UC emission spectrum of $NaMnF_3$: Yb^{3+}, Er^{3+} (50/25/25 mol%); b) Room temperature UC emission spectrum of $NaMnF_3$: Yb^{3+},Tm^{3+} NPs (50/45/5 mol%) dispersed in chloroform (1 mg/ml), spectrum was recorded at a power of 1 w. Pure red and NIR-NIR emission were achieved; c) Proposed energy transfer mechanism of the $NaMnF_3$:Yb^{3+}, Er^{3+} NCs and d) Proposed energy transfer mechanism of the $NaMnF_3$:Yb^{3+}, Tm^{3+} NCs.

3. TUNING MRI T_1 AND T_2 CONTRAST

In MRI, two different imaging modes with specific contrast agents are used and these contrast agents in MRI exhibit either "positive" or "negative" contrast. Gd^{3+} ion is primarily used as T_1 contrast agent due to its seven unpaired electrons in its 4f-orbitals and relatively long electronic relaxation. Its contrast properties are dependent on two factors: the water-exchange rate between bulk water and water bound to the Gd^{3+} ions and the rotational correlation time of the Gd^{3+} containing entities.[13, 14, 24] Most of the Gd^{3+} complexes are chelated with some ligands to reduce the toxicity of the metal.[14] Of the six clinically approved contrast agents used worldwide for intravenous administration, four of them are Gd^{3+}-based chelates.[25] Gd-DTPA complex, for example, has found applications in detecting the disruption of the blood brain barrier and the degree of vascularity, flow dynamics and vascular perfusion.[14] Despite significant achievements in the development of Gd^{3+}-chelate, Gd^{3+}-based NCs are now currenty ardently investigated as they exhibit stronger positive contrast enhancement, better pharmacokinetic parameters and a better control of biodistribution than those of Gd^{3+} complexes. Recently, we developed ultrasmall Gd_2O_3 nanorods and they showed comparable T_1 MRI contrast to commercial T_1 materials (Figure 3).[26] Other types of contrast agents, such as GdF_3 and $NaGdF_4$ NCs, have also been prepared as T_1 contrast agent in MRI.[27, 28] These NCs have increased number of Gd^{3+} per contrast agent and hence increased MRI sensitivity.

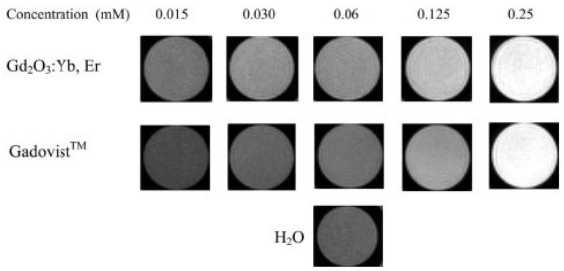

Figure 3. T_1-weighted images of Gd_2O_3:Yb^{3+},Er^{3+} and Gadovist at various Gd^{3+} concentrations. T_1-weighted image of water sample is shown as reference.

Dy^{3+} ion, another type of lanthanide element, have proven to efficiently induce T_2 contrast due to its shorter electronic relaxation time (~ 0.5 ps) and higher magnetic moment (10.6 μ_B).[15, 29] For example, Elst et al. examined Dy-DTPA derivatives as contrast agents in fields between 0.47 and 18.8 T.[30] NCs, such as Dy_2O_3, $Dy(OH)_3$ and $NaDyF_4$, have also been investigated as negative contrast agents in high-field MRI (from 7 to 17.6 T).[31-34] In our recent study, we have reported ultrasmall Dy_2O_3 NCs as positive T_2 contrast agents (r_2 of 2.12 $mM^{-1}s^{-1}$), as shown in Figure 4.[35] This r_2 value, compared with other T_2 contrast agents, is much smaller, which indicated that the NCs possessed relatively large T_2relaxation time.[16, 36] Contrast agents show both T_1 and T_2 relaxation but to a different extent. T_1-weighted positve contrast agents, for example, demonstrated both T_1 and T_2 relaxation properties, but shortening of T_1 relaxation is dominated over that of T_2 relaxation. This results in the image being brighter within areas where the agents are taken up, However, species with high T_1 values lend themselves to darker images.[13] Similarly, T_2-weighted negative contrast influences the signal intensity by shortening T_2, thereby producing darker images while high T_2 results in brightness of the image. This bright T_2 contrast agent is advantageous considering the poor contrast to noise from normal T_2 negative agents in organs such as liver, spleen or in tumors which have inherent low background signal.[16]

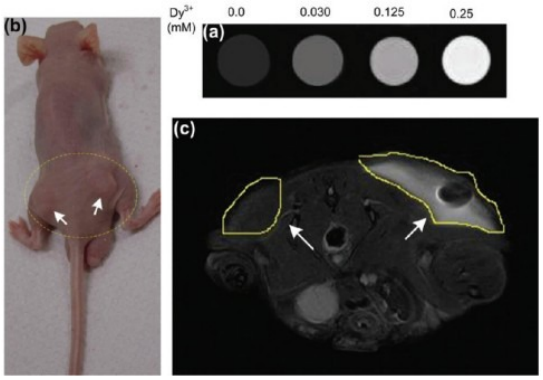

Figure 4. (a) T_2-weighted MR images of silanized Dy_2O_3:Tb NCs in 1% agarose gel with increasing concentrations (0, 0.030, 0.125, 0.25 mM) from left to right. (b) Photograph of a nude mouse implanted with breast tumor (MCF-7) cells. The tumor region is marked by a yellow circle while right and left arrows indicate the positions of the two tumors. (c) The *in vivo* T_2-weighted MR image of tumor regions. The positive contrast arising from Dy_2O_3 NCs is clearly seen at the injection site (right arrow) while the tumor (left arrow) serves as a reference, where no NCs were injected.

Conventional contrast agents respond only to a single imaging mode. They sometimes exhibit ambiguities in MR images, especially when imaging small biological targets. A dual-mode imaging strategy, where T_1 and T_2 MR imaging modes can be utilized simultaneously, has the potential to obtain more comprehensive diagnostic information.[37] For such purpose, Gd^{3+}-labeled magnetite NPs were reported as dual-contrast agents for T_1- and T_2-weighted MR imaging.[38] A "magnetically decoupled" $MnFe_2O_3$-$Gd_2O(CO_3)_2$ core/shell NCs were designed as the dual-contrast agents.[39] Ultrasmall superparamagnetic iron oxide (USPIO) NPs, capable of depicting enhanced T_1 at low concentration range and weak T_2 contrast effects, have been developed.[40] FeCo-graphitic system has also exhibited high T_1 and T_2 contrast effect. However, a thorough understanding of the mechanism by which these systems operate is still unclear.[41]

We have developed a new strategy to achieve tunable T_1-T_2 dual-mode MR contrast and UC fluorescence within a single NC, of which all functionalities arise solely from lanthanide ions. This type of NC has the potnetial to deliver more comprehensive diagnostic information. The $NaDyF_4$:Yb^{3+} seed particles were first prepared, which underwent further growth in a second reaction in the presence of Gd^{3+}, Yb^{3+} and Er^{3+} to form nanorods. The relaxivity of Dy^{3+} ions in the inner shell primarily originates from its magnetization and Curie Spin (CS) relaxation mechanism which becomes very dominant at high magnetic field (Figure 5C).[42, 43] According to the CS relaxation mechanism, the induced Curie magnetic moment per Dy^{3+} ion is given by: $\mu_C = \mu_S^2 B_0/3kT$; where μ_S is the magnetic moment, k is Boltzmann's constant and T is the absolute temperature. This implies that induced magnetization of the Dy^{3+} ions increases with external magnetic field and is proportional to the square of the magnetic moment of Dy^{3+} ions. Gd^{3+} ions on the outer layer of NCs efficiently induce electron-nuclear dipolar interactions with the surrounding water protons, hence shortening the longitudinal relaxation time (T_1) and generating T_1 MRI contrast. Interestingly, tunable positive and negative T_1 enhancement can be achieved by suitably employing a magnetization preparation module in a gradient echo (GE) or a spin echo (SE) sequence. In Figure 5A**,** the images were acquired with a GE T_1-weighted sequence with a magnetization preparation

(inversion pulse) module which exhibits a genuine T_1 contrast (positive enhancement). However, Figure 5B shows T_1-weighted images acquired with a SE sequence without any preparation module, which clearly shows negative enhancement. The current NCs have the advantage of showing tunable properties of positive and negative T_1 by applying appropriate pulse sequences, as well as negative T_2 MRI contrast. Depending on the tissue site of interest, the current NCs can be selectively tuned to enhance imaging contrast by bright or dark T_1 and T_2-weighted MRI in order to achieve complementary information that cannot be obtained by using single mode contrast agents.

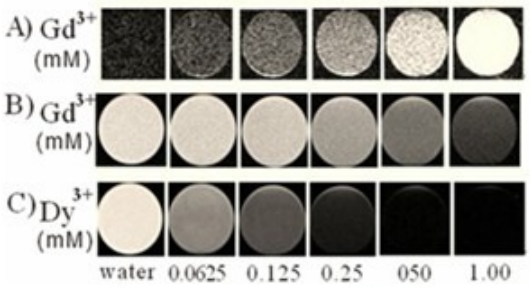

Figure 5. (A) Bright T_1–weighted MR images using gradient echo sequence, (B) dark T_1–weighted images using spin echo sequence and (C) T_2–weighted images of $NaDyF_4:Yb^{3+}$/ $NaGdF_4:Yb^{3+},Er^{3+}$ NCs at different concentrations (0, 0.0625, 0.125, 0.50, 1.00 mM).

4. APPLICATION OF LANTHANIDE NANOCRSTALS IN NANOMEDICINE

Lanthanide NCs have found potential applications in medicine, mainly in drug delivery, diagnostics and cancer cell ablation. [7, 9, 10, 44] NIR-induced drug release and cancer cell ablation using up-converting NCs have generated much interest because NIR radiation is safe to the body and can penetrate deeper into tissues. In one of our works, the UC emissions of $NaYF_4:Yb^{3+},Tm^{3+}$ in the blue region were tuned and further excite to form electron-hole pairs in the nitrogen-doped TiO_2 under 980 nm irradiation and thereby create ROS, as discussed in section 2.[20] TiO_2 NPs are good candidates for drug delivery and cancer therapy owing to their high reactivity, high stability, non-toxicity and low costs. Existing reported works involving TiO_2 on cancer therapy and drug release demonstrated the principle of electron-hole pairs formation in TiO_2 under UV light irradiation and thereby create highly reactive ROS.[45] ROS can damage the cancer cell membrane and induce programmed cancer cell death, while in drug release, ROS can sever the hydrocarbon chains attached on the surface of TiO_2 and thus leads to the release of drug.[46] Using NIR irridation instead of UV light eliminates intrinsic problems associated direct UV or blue irradiation onto biological specimens. The mechanism of the targeted cancer cell ablation of using N-TiO_2/$NaYF_4$:Yb,Tm nanocomposites is shown in Figure 6. Briefly, NIR-induced excitation generates blue emission from the core $NaYF_4$:Yb,Tm, which in turn excites the N-TiO_2 in the shell, generating ROS.

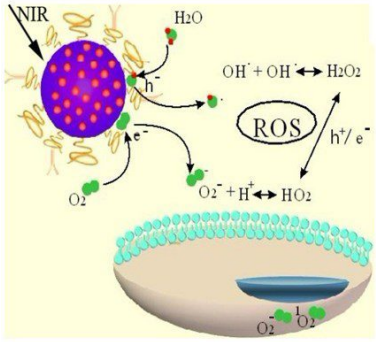

Figure 6. Diagram showing the mechanism of cancer cells killing of the N-TiO_2/$NaYF_4$:Yb,Tm nanocomposites upon irradiation with 980 nm laser.

The formation of hydroxyl radicals is cruical to generate ROS. To prove the generation of hydroxyl radicals, a fluorescence analytical technique based on a terephalic acid (TA) reaction was employed.[47, 48] The fluorescence intensity gradually increased with the increase of irradiation time and the generation of strong blue fluorescence upon excitation at 320 nm proved the formation of OH• radicals (Figure 7a). NIR-induced drug release property of this system was measured using a model drug (7-methoxycoumarin-3-carboxylic acid). Under NIR irradiation, cleaving took place at the anchoring groups and caused the model drug releasing into deionised (DI) water (Figure 7b).[49] Before NIR irradiation, there was no fluorescence observed, indicating that no dye was released. After NIR irradiation, a strong blue fluorescence of high intensity peak at 405 nm (excitation wavelength 320 nm) was observed, which proved the release of the model drug into DI water under NIR irradiation (Figure 7b inset). Anti-cAngptl4 Ab-conjugated nanocomposites were demonstrated in triggered cancer cell ablation (Figure 7c). Fluorescence Activated Cell Sorting (FACS) analysis (Figure 7c) showed a slight increase in apoptotic A-5RT3 cells (Annexin V+/PI+ and Annexin V+/PI-) when treated with anti-cAngptl4 Ab nanoparticles when compared with unconjugated nanoparticles, even in the absence of NIR exposure (unconjugated vs anti-cAngptl4-conjugated: 7.53 % vs 13.67 %). Upon NIR exposure, anti-cAngptl4 Ab-NCs treated A-5RT3 showed a further ~2.5-fold increase (31.49 %) in apoptotic cells. Although there was a slight increase in the percentage of apoptotic cells in NIR exposed unconjugated NCs treated A-5RT3 (9.8 %), this difference was not statistically significant. FACS analysis also showed no significant difference in the percentage of apoptotic HaCaT cells treated with unconjugated nanoparticles regardless of NIR exposure, suggesting that the NCs exerted their cytotoxic effects only in close proximity to the cells. This study shows that the functionalization of the NCs with anti-cAngptl4 antibody conferred selective anti-tumor property, which is activated/triggered by NIR irradiation

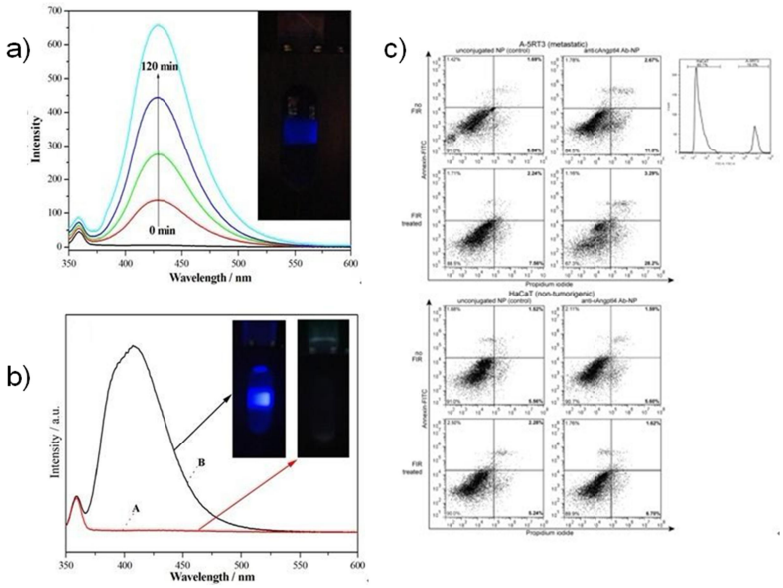

Figure 7. a) Time-dependent fluorescence spectra of the terephthalic acid solution (8 X 10^{-4} M) containing 10 mg of N-TiO_2/$NaYF_4$:Yb,Tm upon 980 nm irradiation. Inset: photographs show the light emission of the 2-hydroxyterephthalic acid solution after NIR irradiation; b) Fluorescence spectra of the 7-methoxycoumarin-3-carboxylic acid solution released from N-TiO_2/$NaYF_4$:Yb,Tm A) before and B) after NIR irradiation. Inset: photographs show the light emission of the 7-methoxycoumarin-3-carboxylic acid solution before and after NIR irradiation, respectively; c) FACS analysis of apoptotic A-5RT3 cells (Annexin V^+/PI^+ and Annexin V^+/PI^-) when treated with anti-cAngptl4 Ab nanoparticles and unconjugated nanoparticles, in and in the absence of NIR exposure. Percentage of apoptotic cells before and after NIR exposure as analyzed by FACS (10,000 events). The sum of Annexin V+/PI- (early apoptosis) and Annexin V+/PI+ cells (late apoptosis) were considered apoptotic. Metastatic A-5RT3 cells were prelabeled with Cell Tracker Blue CMAC. Representative dot plots from n=5 independent studies were shown.

5. CONCLUSIONS

There has been significant advancements involving lanthanide nanomaterials for nanomedicine, particularly when multifunctional and hybrid platforms were employed. However, many challenges still remain and issues are to be resolved before these NCs can be translated to clinical application.[50] Determination of the long-term toxicity of the NCs

is still one of the main hurdles that require the establishment of standards and testing protocols that can provide benchmarks for the development of novel classes of materials including lanthanide materials.[51] The lack of *in vivo* studies involving lanthanide nanomaterials means that there is limited information about the long-term efficacy and health implications of using these products. Limited *in vitro* studies focused on toxicology of lanthanide nanomaterials showed that the concentration of lanthanide metals will affect the upregulation of inflammatory genes, whilst the type of assay methods used to assess cytotoxicity needs to be optimized.[52] In addition, further studies need to be carried out to evaluate the post exposure effects of lanthanide nanomaterials on cell biology and physiology.

ACKNOWLEDGEMENTS

This work was supported by Singapore Ministry of Education AcRF Tier 2ARC 16/11.

REFERENCES

[1] Riehemann, K.; Schneider, S. W.; Luger, T. A.; Godin, B.; Ferrari, M.; Fuchs, H., "Nanomedicine - Challenge and perspectives," Angew. Chem. Int. Ed. 48 (5), 872-897 (2009).
[2] Peer, D.; Karp, J. M.; Hong, S.; Farokhzad, O. C.; Margalit, R.; Langer, R., "Nanocarriers as an emerging platform for cancer therapy," Nat. Nanotech. 2 (12), 751-760 (2007).
[3] Boisselier, E.; Astruc, D., "Gold nanoparticles in nanomedicine: Preparations, imaging, diagnostics, therapies and toxicity," Chem. Soc. Rev. 38 (6), 1759-1782 (2009).
[4] Zhang, L.; Gu, F. X.; Chan, J. M.; Wang, A. Z.; Langer, R. S.; Farokhzad, O. C., "Nanoparticles in medicine: Therapeutic applications and developments," Clin. Pharmacol. Therap. 83 (5), 761-769 (2008).
[5] Weissleder, R.; Ntziachristos, V., "Shedding light onto live molecular targets," Nat. Med. 9 (1), 123-128 (2003).
[6] Massoud, T. F.; Gambhir, S. S.," Molecular imaging in living subjects: Seeing fundamental biological processes in a new light," Genes Devel. 17 (5), 545-580 (2003).
[7] Ntziachristos, V.; Bremer, C.; Weissleder, R., "Fluorescence imaging with near-infrared light: New technological advances that enable in vivo molecular imaging," Eur. Radiology 13 (1), 195-208 (2003).
[8] Torchilin, V. P., "Multifunctional nanocarriers," Adv. Drug Delivery Rev. 58 (14), 1532-1555 (2006).
[9] Wang, F.; Liu, X., "Recent advances in the chemistry of lanthanide-doped upconversion nanocrystals," Chem. Soc. Rev. 38 (4), 976-989 (2009).
[10] Wang, F.; Banerjee, D.; Liu, Y.; Chen, X.; Liu, X., "Upconversion nanoparticles in biological labeling, imaging, and therapy," Analyst 135 (8), 1839-1854 (2010).
[11] Aime, S.; Crich, S. G.; Gianolio, E.; Giovenzana, G. B.; Tei, L.; Terreno, E., "High sensitivity lanthanide(III) based probes for MR-medical imaging," Coord. Chem. Rev. 250 (11-12), 1562-1579 (2006).
[12] Strijkers, G. J.; Mulder, W. J. M.; van Tilborg, G. A. F.; Nicolay, K., "MRI contrast agents: Current status and future perspectives," Anti-Cancer Agents Med. Chem. 7 (3), 291-305 (2007).
[13] Bottrill, M.; Kwok, L.; Long, N. J., "Lanthanides in magnetic resonance imaging," Chem. Soc. Rev. 35 (6), 557-571 (2006).
[14] Laurent, S.; Vander Elst, L.; Muller, R. N., "Lanthanide complexes for magnetic resonance and optical molecular imaging," Quarterly J. Nucl. Med. Molec. Imaging 53 (6), 586-603 (2009).
[15] Vander Elst, L.; Zhang, S.; Sherry, A. D.; Laurent, S.; Botteman, F.; Muller, R. N., "Dy-complexes as high field T2 contrast agents: Influence of water exchange rates," Academic Radiol. 9 (SUPPL. 2), S297-S299 (2002).
[16] Corot, C.; Robert, P.; Idée, J. M.; Port, M., "Recent advances in iron oxide nanocrystal technology for medical imaging," Adv. Drug Delivery Rev. 58 (14), 1471-1504 (2006).
[17] Jüstel, T.; Nikol, H.; Ronda, C., "New developments in the field of luminescent materials for lighting and displays," Angew. Chem. Inter. Ed. 37 (22), 3084-3103 (1998).
[18] Mader, H. S.; Kele, P.; Saleh, S. M.; Wolfbeis, O. S., "Upconverting luminescent nanoparticles for use in bioconjugation and bioimaging," Curr. Opin. Chem. Biol. 14 (5), 582-596 (2010).
[19] Haase, M.; Schäfer, H., "Upconverting nanoparticles," Angew. Chem. Int. Ed.50 (26), 5808-5829 (2011).
[20] Xu, Q.C., Zhang,Y., Tan, M. J. , Liu, Y. , Yuan, S., Cleo,C. , Tan, N.S., Tan, T. Y. T., "Anti-cAngptl4 Ab-conjugated N-TiO_2/$NaYF_4$:Yb,Tm Nanocomposite for Near Infrared-Triggered Drug Release and Enhanced Targeted Cancer Cell Ablation," Adv. Healthcare Mater. 1 (4), 470-472 (2012).
[21] Wang, J.; Wang, F.; Wang, C.; Liu, Z.; Liu, X., "Single-Band Upconversion Emission in Lanthanide-Doped $KMnF_3$ Nanocrystals," Angew. Chem. Inter. Ed. 50 (44), 10369-10372 (2011).

[22] Tian, G.; Gu, Z.; Zhou, L.; Yin, W.; Liu, X.; Yan, L.; Jin, S.; Ren, W.; Xing, G.; Li, S.; Zhao, Y., "Mn^{2+} Dopant-Controlled Synthesis of $NaYF_4$:Yb/Er Upconversion Nanoparticles for in vivo Imaging and Drug Delivery," Adv.Mater. 24 (9), 1226-1231 (2012).
[23] Zhang, Y.; Lin, J. D.; Vijayaragavan, V.; Bhakoo, K. K.; Tan, T. T. Y., "Tuning sub-10 nm single-phase $NaMnF_3$ nanocrystals as ultrasensitive hosts for pure intense fluorescence and excellent T_1 magnetic resonance imaging," Chem. Commun. 48 (83), 10322-10324 (2012).
[24] Caravan, P., "Strategies for increasing the sensitivity of gadolinium based MRI contrast agents," Chem. Soc. Rev. 35 (6), 512-523 (2006).
[25] Bottrill, M., Kwok, L., Long, N. J., "Lanthanides in magnetic resonance imaging," Chem. Soc.Rev. 35 (6), 557-571 (2006).
[26] Das, G. K.; Heng, B. C.; Ng, S. C.; White, T.; Loo, J. S. C.; D'Silva, L.; Padmanabhan, P.; Bhakoo, K. K.; Selvan, S. T.; Tan, T. T. Y., "Gadolinium oxide ultranarrow nanorods as multimodal contrast agents for optical and magnetic resonance imaging," Langmuir 26 (11), 8959-8965 (2010).
[27] Evanics, F.; Diamente, P. R.; Van Veggel, F. C. J. M.; Stanisz, G. J.; Prosser, R. S., "Water-soluble GdF3 and GdF_3/LaF_3 nanoparticles - Physical characterization and NMR relaxation properties," Chem. Mater. 18 (10), 2499-2505 (2006).
[28] Park, Y. I.; Kim, J. H.; Lee, K. T.; Jeon, K. S.; Na, H. B.; Yu, J. H.; Kim, H. M.; Lee, N.; Choi, S. H.; Baik, S. I.; Kim, H.; Park, S. P.; Park, B. J.; Kim, Y. W.; Lee, S. H.; Yoon, S. Y.; Song, I. C.; Moon, W. K.; Suh, Y. D.; Hyeon, T., "Nonblinking and nonbleaching upconverting nanoparticles as an optical imaging nanoprobe and T_1 magnetic resonance imaging contrast agent," Adv. Mater. 21 (44), 4467-4471 (2009).
[29] Caravan, P.; Greenfield, M. T.; Bulte, J. W. M., "Molecular factors that determine Curie spin relaxation in dysprosium complexes," Magn. Reson. Med. 46 (5), 917-922 (2001).
[30] Vander Elst, L.; Roch, A.; Gillis, P.; Laurent, S.; Botteman, F.; Bulte, J. W. M.; Muller, R. N., "Dy-DTPA derivatives as relaxation agents for very high field MRI: The beneficial effect of slow water exchange on the transverse relaxivities," Magn. Reson. Med. 47 (6), 1121-1130 (2002).
[31] Norek, M.; Kampert, E.; Zeitler, U.; Peters, J. A., "Tuning of the size of Dy_2O_3 nanoparticles for optimal performance as an MRI contrast agent," J. Am.Chem. Soc. 130 (15), 5335-5340 (2008).
[32] Kattel, K.; Park, J. Y.; Xu, W.; Kim, H. G.; Lee, E. J.; Bony, B. A.; Heo, W. C.; Jin, S.; Baeck, J. S.; Chang, Y.; Kim, T. J.; Bae, J. E.; Chae, K. S.; Lee, G. H., "Paramagnetic dysprosium oxide nanoparticles and dysprosium hydroxide nanorods as T_2 MRI contrast agents," Biomaterials 33 (11), 3254-3261 (2012).
[33] Zhang, Y.; Vijayaragavan, V.; Das, G. K.; Bhakoo, K. K.; Tan, T. T. Y., "Single-phase $NaDyF_4$:Tb^{3+} nanocrystals as multifunctional contrast agents in high-field magnetic resonance and optical imaging," Eur. J. Inorg. Chem. (12), 2044-2048 (2012).
[34] Das, G. K.; Johnson, N. J. J.; Cramen, J.; Blasiak, B.; Latta, P.; Tomanek, B.; Van Veggel, F. C. J. M., "$NaDyF_4$ nanoparticles as T_2 contrast agents for ultrahigh field magnetic resonance imaging," J. Phys.Chem. Lett. 3 (4), 524-529 (2012).
[35] Das, G. K.; Zhang, Y.; D'Silva, L.; Padmanabhan, P.; Heng, B. C.; Chye Loo, J. S.; Selvan, S. T.; Bhakoo, K. K.; Yang Tan, T. T., "Single-phase Dy_2O_3:Tb^{3+} nanocrystals as dual-modal contrast agent for high field magnetic resonance and optical imaging," Chem. Mater. 23 (9), 2439-2446 (2011).
[36] Bulte, J. W. M.; Kraitchman, D. L., "Iron oxide MR contrast agents for molecular and cellular imaging," NMR Biomed. 17 (7), 484-499 (2004).
[37] Hu, F.; Zhao, Y. S., "Inorganic nanoparticle-based T_1 and T_1/T_2 magnetic resonance contrast probes," Nanoscale 4 (20), 6235-6243 (2012).
[38] Bae, K. H.; Kim, Y. B.; Lee, Y.; Hwang, J. Y.; Park, H.; Park, T. G., "Bioinspired synthesis and characterization of gadolinium-labeled magnetite nanoparticles for dual contrast T_1- and T_2-weighted magnetic resonance imaging," Bioconjugate Chem. 21 (3), 505-512 (2010).
[39] Choi, J. S.; Lee, J. H.; Shin, T. H.; Song, H. T.; Kim, E. Y.; Cheon, J., "Self-confirming "AND" logic nanoparticles for fault-free MRI," J. Am. Chem. Soc. 132 (32), 11015-11017 (2010).
[40] Corot, C.; Robert, P.; Idée, J.-M.; Port, M., "Recent advances in iron oxide nanocrystal technology for medical imaging," Adv. Drug Delivery Rev. 58 (14), 1471-1504 (2006).
[41] Seo, W. S.; Lee, J. H.; Sun, X.; Suzuki, Y.; Mann, D.; Liu, Z.; Terashima, M.; Yang, P. C.; McConnell, M. V.; Nishimura, D. G.; Dai, H., "FeCo/graphitic-shell nanocrystals as advanced magnetic-resonance-imaging and near-infrared agents," Nat. Mater. 5 (12), 971-976 (2006).

[42] Norek, M.; Peters, J. A., "MRI contrast agents based on dysprosium or holmium," Prog. Nucl. Magn. Reson. Spectros. 59 (1), 64-82 (2011).
[43] Viswanathan, S.; Kovacs, Z.; Green, K. N.; Ratnakar, S. J.; Sherry, A. D., "Alternatives to gadolinium-based metal chelates for magnetic resonance imaging," Chem. Rev. 110 (5), 2960-3018 (2010).
[44] Selvin, P. R.,"Principles and biophysical applications of lanthanide-based probes," Annu. Rev. Biophys. Biomol. Struct. 31, 275-302 (2002).
[45] Rozhkova, E. A.; Ulasov, I.; Lai, B.; Dimitrijevic, N. M.; Lesniak, M. S.; Rajh, T., "A High-Performance Nanobio Photocatalyst for Targeted Brain Cancer Therapy," Nano Lett. 9 (9), 3337-3342 (2009).
[46] Song, Y.-Y.; Schmidt-Stein, F.; Bauer, S.; Schmuki, P., "Amphiphilic TiO_2 Nanotube Arrays: An Actively Controllable Drug Delivery System," J. Am. Chem. Soc. 131 (12), 4230-4232 (2009).
[47] Li, C.; Wang, F.; Zhu, J.; Yu, J. C., "$NaYF_4$:Yb,Tm/CdS composite as a novel near-infrared-driven photocatalyst," Appl. Catal. B 100 (3–4), 433-439 (2010).
[48] Hirakawa, T.; Nosaka, Y., "Properties of O2•- and OH• formed in TiO_2 aqueous suspensions by photocatalytic reaction and the influence of H_2O_2 and some Ions," Langmuir 18 (8), 3247-3254 (2002).
[49] Balaur, E.; Macak, J. M.; Taveira, L.; Schmuki, P., "Tailoring the wettability of TiO_2 nanotube layers," Electrochem. Comm. 7 (10), 1066-1070 (2005).
[50] Sanhai, W. R.; Sakamoto, J. H.; Canady, R.; Ferrari, M., "Seven challenges for nanomedicine," Nat. Nanotechnol. 3 (5), 242-244 (2008).
[51] Vega-Villa, K. R.; Takemoto, J. K.; Yáñez, J. A.; Remsberg, C. M.; Forrest, M. L.; Davies, N. M., "Clinical toxicities of nanocarrier systems," Adv. Drug Delivery Rev. 60 (8), 929-938 (2008).
[52] Drynda, A.; Deinet, N.; Braun, N.; Peuster, M., "Rare earth metals used in biodegradable magnesium-based stents do not interfere with proliferation of smooth muscle cells but do induce the upregulation of inflammatory genes," J. Biomed. Mater. Res. Part A 91 (2), 360-369 (2009).